https://doi.org/10.1016/j.buildenv.2019.106533

Experimental study on convective heat transfer coefficients for the human body exposed to turbulent wind conditions

Yichen Yu[a], Jianlin Liu[b,*], Kapil Chauhan[c], Richard de Dear[a], Jianlei Niu[a, c, d]

[a] School of Architecture, Design and Planning, The University of Sydney, NSW, Australia

[b] College of Environmental Science and Engineering, Donghua University, Shanghai, P. R. China

[c] Centre for Wind, Waves and Water, School of Civil Engineering, The University of Sydney, NSW, Australia

[d] Department of Building Services Engineering, The Hong Kong Polytechnic University, Hung Hom, Kowloon, Hong Kong

*Corresponding author: jian-lin.liu@connect.polyu.hk

Abstract

Ongoing urbanization and urban densification are leading to an increasing number of tall buildings, giving rise to an increasingly complex urban morphology which, in turn, is complicating the pedestrian-level wind environment of urban areas. As a key climatic element determining pedestrian outdoor thermal comfort, wind is represented in most of the existing outdoor comfort models, but its effects have been oversimplified to date. This study aims to examine how wind velocity and turbulence intensity affect convective heat loss over a human body. A wind tunnel with a turbulence-grid is used to simulate outdoor wind flow with turbulence intensity ranging from 13% to 36%, and wind velocity from 0.7 m/s to 6.7m/s. Forced convective heat transfer loss for individual body segments have been measured on a

thermal manikin using a constant skin temperature regulation mode. Results for unit effect confirm that convective heat loss increases with turbulence intensity, which prompts us to make explicit the turbulence intensity when calculating the heat loss from human body. Ignoring turbulence causes the impact of wind on pedestrian thermal sensation to be underestimated by up to 50%. Based on the present data, regression formula derived from regular geometry for predicting convective heat transfer coefficients has been expanded to serve individual body segments. Accounting for the effect of both wind velocity and turbulence intensity, the accuracy of convective heat loss calculation in outdoor thermal comfort research would be improved.

Keywords: Convective heat transfer coefficient; Turbulence intensity; Wind tunnel experiments; Thermal manikin; Outdoor thermal comfort

1. Introduction

Multiple disciplines are working together to develop a more productive, sustainable, and liveable city. An increasingly important issue is the urban heat island effect, which not only restricts daily activity options but also leads to an increase in number of people hospitalised with heat-related illnesses [1-3]. Heat-related morbidity and mortality in urban areas may be ameliorated with a better understanding of their thermal-physiological climate. Thermal comfort is a subjective evaluation of the environment, a combined result of the interaction of heat exchange with the surrounding environment and physiological regulation of bodily heat content [4, 5]. Over the last century, researchers have created several thermal comfort models that mathematically describe the thermoregulation processes and predict human thermal responses to different combinations of indoor thermal environmental parameters (including air temperature, humidity, radiation, wind speed) and personal variables (clothing and activity levels) [6-9].

Attempts at re-purposing these indoor thermal comfort models to the outdoor context have been less than satisfactory, with several field studies reporting significant discrepancies between the onsite questionnaire responses from human subjects and thermal comfort model predictions using the same meteorological exposures. In particular, the models fail to adequately reflect pedestrians' hypersensitivity to dynamic urban wind conditions [10-12].

Outdoor wind environments are normally characterized by inhomogeneous and transient changes in terms of several environmental parameters [13], complex in both space and time. In space, the pedestrian-level wind environment (below 2 m) is in the urban canopy layer, where its climate is an amalgam of microclimatic effects superimposed on regional scale synoptic-scale meteorological conditions by the immediate surroundings [14, 15]. Field experiments and simulation studies both confirm that wind is easily governed by types of topography and terrain surface characteristics [16-18]. In time-frequency analysis, wind contains far more information than just mean velocity, including but not limited to turbulence intensity (the turbulence amplitude of the airflow), integral length scale (magnitude of most frequent and dominant vortex inside the turbulent eddy), and power spectral density (the distribution of power at the different frequencies) [19]. Among these characteristics of wind flow, turbulence intensity has been demonstrated to have a mechanical and thermal impact on the human body. The mechanical power is related to the dynamic pressure. Hunt et al. [20] performed a series experiment in the wind tunnel to test how wind-induced mechanical force at different turbulence level affect the performance of everyday tasks, and proposed a concept of "equivalent steady wind velocity (v_s)" (Eq. 1), which has a similar effect to a low-speed turbulent wind .

$$v_s = v_d(1 + 3 * TI) \quad (1)$$

where v_d is the dynamic wind velocity (m/s), v_s is the equivalent steady wind velocity (m/s), TI is the turbulence intensity (%).

There are two explanations suggested for the thermal effects of dynamic airflow on humans. The first, raised by Mayer [21], suggests that the convective heat loss increases with turbulence intensity, which in turn reduces the local skin temperature of the human body. This has been tested experimentally on a heated head manikin placed inside a controlled environmental chamber, with the wind velocity below 0.5 m/s, and the turbulence intensity ranging from 14% to 55% [22, 23]. Based on the experimental results, the convective heat transfer has been presented as a function of the product of velocity and turbulence intensity. The second explanation has been proposed by Fanger [24, 25] and suggests that higher turbulence intensity does not decrease the mean level of skin temperature but instead causes stronger temperature fluctuations which, in turn, trigger greater cutaneous thermoreceptor activity than under steady air flows at the same mean velocity. Following this, a semi-empirical draft risk model (Eq. 2) has been developed using air temperature, air velocity and turbulence intensity as inputs [24].

$$PD = 3.143(34 - T_a)(u - 0.05)^{0.6223} + 0.3696 * u * TI(34 - T_a)(u - 0.05)^{0.6223} \quad (2)$$

where, PD is the predicted percentage of dissatisfaction caused by draught, T_a is the air temperature, TI is turbulence intensity, and u is the mean air velocity.

Therefore, based on the above-mentioned studies, a primary goal of the present paper is to qualify the effect of turbulence intensity on heat transfer over different anatomical body segments. The forehead data examined in Mayer's experiment [21] is unrepresentative of the condition of the entire body, and the range of wind velocities he investigated is not large enough to extrapolate to outdoor settings. A full-size thermal manikin has proven to be an effective instrument to measure sensible heat transfer between human body surface and the surrounding

environment in environmental ergonomics [26]. It features an anatomically realistic human morphology, with a precision heating element and temperature sensor system embedded within the "skin." Wyon et al. [27] suggested the use of thermal manikin as the most effective instrument to evaluate complex thermal environments. They proposed a manikin-based temperature index (Equivalent Homogeneous Temperature, EHT) of a hypothetical, isothermal environment with no wind that would cause the same dry heat loss from individual body segments as in the actual, complex, and windy environment, thereby making the manikin's results more intuitive and easier to communicate. Tanabe et al. [28] specified the logic and utility of a comfort skin temperature control mode for the thermal manikin and calculated the manikin-based EHT to evaluate complex thermal environments. On the other hand, de Dear et al. [29] was the first to measure separately radiative (h_r) and convective heat transfer coefficients (h_c) on individual body segments in a wind tunnel, covering most of the daily outdoor wind speed ranges. To fit stronger wind conditions, Li.et al [30] broadened the test scope to include wind speeds up to 12.7 m/s. While velocity has been thoroughly investigated in the literature, limited studies have focused on the effects of turbulence intensity to date. Ono et al. [31] performed experiments at a turbulence intensity of approximately 11% and expressed h_c as a function of wind velocity and turbulence intensity. However, there is no clear statement of the principle behind their proposed formula, and the turbulence intensities investigated are not high enough to compare with frequently recorded field measurements (around 30%) for a typical pedestrian-level urban microclimate [19].

This study aims to measure the heat loss from human body surface in simulated outdoor urban wind environments - with realistic turbulence intensity and air velocity ranges. The new predictive equation would effectively improve the accuracy in estimating the convective heat transfer between the body surface and outdoor urban environments.

2. Methodology

2.1. Thermal manikin setup

The present study involves a thermal manikin to quantify the effects of wind velocity and turbulence intensity on the convective heat transfer coefficient over the human body. The manikin was operated at a constant skin temperature control mode and tested in a series of pre-measured wind conditions in the wind tunnel. The convective heat transfer coefficient is calculated based on the thermal state (skin temperature and heat loss) automatically logged by manikin itself and the operative temperature in the wind tunnel measured using the iButton device.

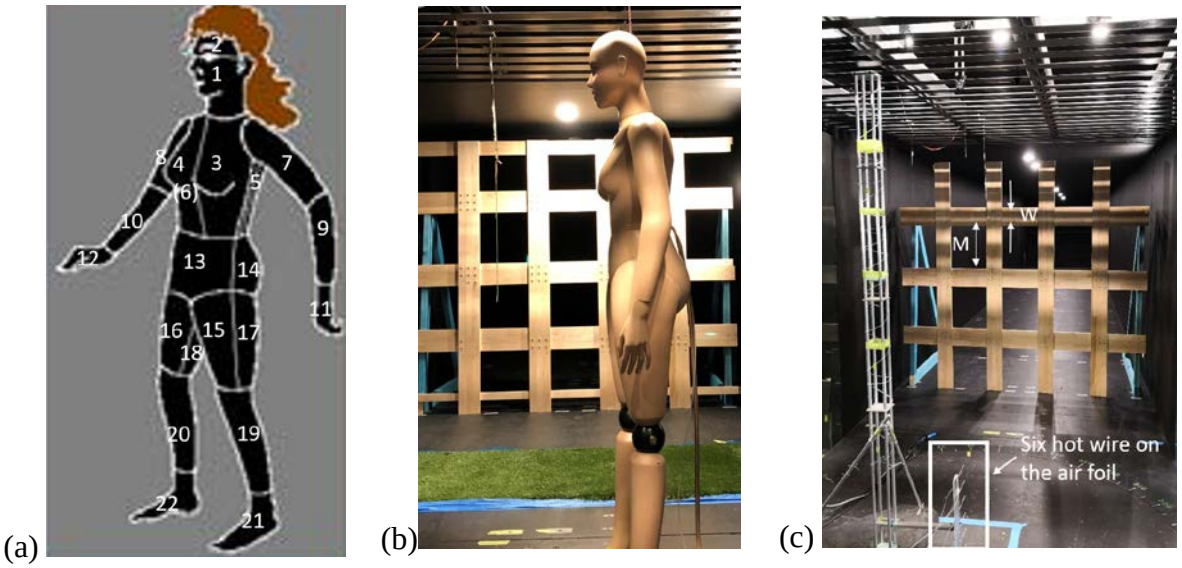

Fig. 1. (a) Manikin's segments indication (the numbers correspond to the first column in Table 1) (b) placement of thermal manikin during the experiment, and (c) wind tunnel set-up for the wind profile measurements.

Table 1
Body area and height of the manikin.

Segment	Area (m^2)	Hotwire anemometer heights corresponding to each body segment (m)	Temperature sensors heights corresponding to each body segments (m)
1.Head	0.090	1.45-1.60	1.7
2.Crown	0.049	1.67-1.74	1.7
3.Chest Left	0.070	1.10-1.40	1.1-1.7
4.Chest Right	0.070	1.10-1.40	1.1-1.7
5.Back Left	0.070	1.10-1.40	1.1-1.7
6.Back Right	0.070	1.10-1.40	1.1-1.7
7.Upper Arm Left	0.074	1.10-1.40	1.1-1.7
8.Upper Arm Right	0.076	1.10-1.40	1.1-1.7
9.Forearm Left	0.050	0.89-1.03	0.9-1.3
10.Forearm Right	0.050	0.89-1.03	0.9-1.3
11.Hand Left	0.038	0.67-0.82	0.5-0.9
12.Hand Right	0.038	0.67-0.82	0.5-0.9
13.Pelvis	0.055	0.89-1.03	0.9-1.3
14.Backside	0.110	0.89-1.03	0.9-1.3
15.Front Thigh Left	0.090	0.53-1.03	0.5-0.9
16.Front Thigh Right	0.090	0.53-1.03	0.5-0.9
17.Back Thigh Left	0.090	0.53-1.03	0.5-0.9
18.Back Thigh Right	0.090	0.53-1.03	0.5-0.9
19.Calf Left	0.098	0.16-0.46	0.1-0.5
20.Calf Right	0.098	0.16-0.46	0.1-0.5
21.Foot Left	0.048	0.02-0.09	0.1
22.Foot Right	0.048	0.02-0.09	0.1
23.Whole Body	1.562	0.02-1.74	0.1-1.7

The thermal manikin comprising 22 individually thermo-regulated anatomical segments, was used in this experiment (Fig. 1a-b). Below the manikin's thermally conductive polyester skin, pure nickel wires were wound around each body part with 2.2 mm spacing between each winding, thereby ensuring uniform heat loss over the entire anatomical section. The standing height of the manikin was 1.7 m and details of the body surface area of each anatomical segment were presented in Table 1. We suspended the unclothed manikin in a standing posture above the turntable of the wind tunnel with a string fastened to the ceiling beam of the tunnel's working section. The manikin was operated in constant skin temperature control mode, and the

pre-setting of skin temperature was set as 12 K higher than the real-time air temperature in the wind tunnel. Under the steady-state condition, the heat supplied to each of the manikin's segments equalled its sensible heat loss to the surrounding environment. The segmental skin temperature was continuously logged at 40 Hz frequency, and the heat loss was updated eight times per second.

2.2. Wind Tunnel Setup

The boundary layer wind tunnel used in this study was 20 m long, 2.5 m wide and 2 m high. To measure the wind profile, we manually moved six hotwire anemometers (DANTEC DYNAMICS miniature wire probe 55P11, calibrated pre-and-post experiment) along a steel frame to span distance between floor and ceiling of the tunnel working section. The sampling frequency for each anemometer was set to 20,000 Hz, with a sampling duration lasting 180 seconds.

The freestream turbulence intensity in the bare tunnel fell below 1% between heights of 0.3 m and 1.8 m (i.e. unaffected by floor and ceiling roughness). For generating high levels of turbulence (*TI* >15%), passive grids were widely used in wind tunnel experiments. The grid turbulence downstream of bars was caused by its subsequent shedding of vortices. The turbulence characteristics depended on the width of the bars (*W*), the mesh size (the distance between the centreline of the bars) (*M*), and the downstream distance (*L*) from the measurement point to the grid [32, 33]. It has been pointed out that the working section should be long enough to ensure that decay is the dominant process- occurs after two to three times of the mesh size behind the grid [32]. Similarly, Baines et al. [34] found that, if the flow is to be uniform, the model could be no closer than five mesh widths from the grid. After that, the ratio *W*/*M* can be chosen based on the definition of the grid drag coefficient (c_D), which recommended to be kept between 3 and 4 [32].

$$c_D = \frac{W/M(2-W/M)}{(1-\frac{W}{M})^4} \quad (3)$$

To further match the size of the wind tunnel, the grid system served in the present study is built up with 0.05m width wooden slats, and formed the mesh size of 0.45m (Fig. 1c).

To test the homogenous of the wind profile in the manikin standing area, three locations were chosen: in the middle of manikin's feet, 0.3m on the left and right sides, respectively. To examine its temporal homogenous, we keep the sampling time for each measurement at 180s, and repeat for three times at three locations. Results show that when L is larger than 2.25m (approximate five times M), the fluctuation of turbulence intensity did not exceed 2.5%.

The inflow air velocity was controlled through the rotational speed of the wind tunnel fan, and different turbulence levels were obtained by adjusting the distance between the measurement point and grid system. The inner wall of the wind tunnel was covered by black paperboard to ensure a homogeneous radiative environment. During the experiment, the wind tunnel was maintained without illumination, so the mean radiant temperature was assumed identical to the air temperature at the test section. Ten 'iButton' temperature sensors (ONSOLUTION, Thermochron, TCS) were distributed on the left and right side of the wall, respectively at 0.1, 0.5, 0.9, 1.3 and 1.7m above the floor, to measure air (and operative) temperature inside the wind tunnel. The operation of wind tunnel fan inevitably released some extra heat into the test section, and the time-averaged temperature during each case was used for the following manikin calculations.

(a)

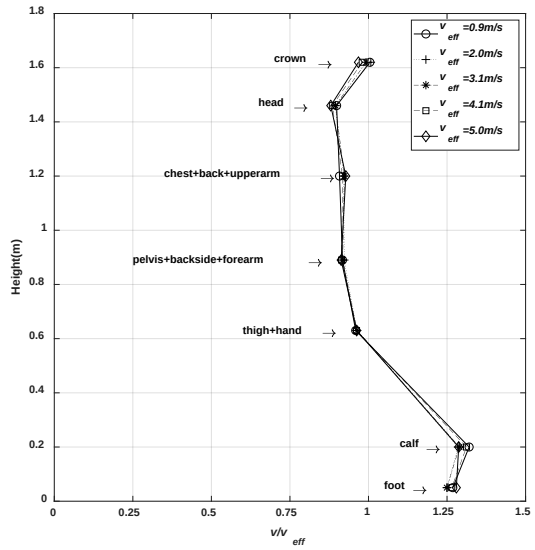

(b)

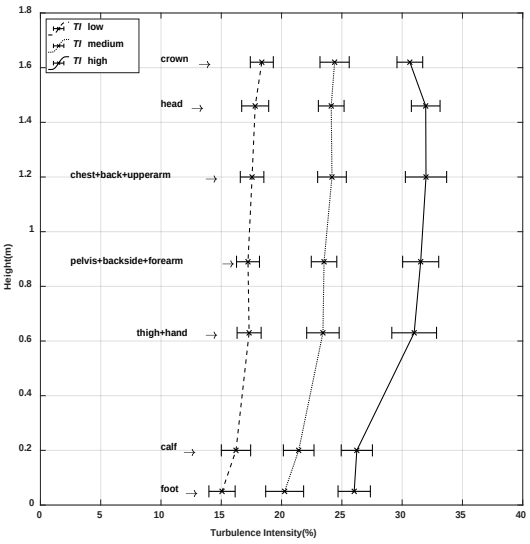

Fig. 2. (a) Normalized wind velocity profile at the height of each body segment, and (b) wind turbulence profile at the height of each body segment.

Fig. 2(a) shows the velocity profile, which is independent of the rotation speed of the fan in range. At the same distance between the measurement point and grid system, the turbulence intensity was quite stable at different velocities, with a discrepancy in the average value less than 2% at each manikin body segment. Due to the inconsistent wind speed distribution across the whole body, we utilized an area weighted mean velocity index v_{eff}, by weighting wind speed experienced by different body segments with their corresponding surface area. Fig. 2(b) shows the distribution of turbulence intensity at the height of each body segment. The vertical average value of *TI* was 17% in the lowest group, 23% in the medium group, and 30% in the highest group. Compared to the large discrepancy in turbulence intensity, wind velocity is relatively stable, with the standard deviation being less than ± 0.2 m/s at all seven measurement heights.

2.3. Determination of the radiative and convective heat transfer coefficients

To obtain h_c at a target wind condition, we measure the radiation heat transfer coefficient h_r and subtract it from the total sensible heat transfer coefficient h. This was first introduced by de Dear et al.'s [29] - covering the manikin skin surface with a low-emissivity coating to separate the radiative and convective heat transfer from the total dry heat loss- which, was adopted in many previous studies with its repeatability testified [35]. Sensible heat loss from the skin to the environment consists of convective (*C*) and Radiative (*R*) heat loss, and is further expressed as the product of the heat transfer coefficient and the corresponding temperature difference [36].

$$Q = C + R = h_c(T_{sk} - T_a) + h_r(T_{sk} - T_r), \quad (4)$$

where Q was total sensible heat flux ($\mathrm{W/m^2}$), C was convective heat flux density ($\mathrm{W/m^2}$), R was radiative heat flux density ($\mathrm{W/m^2}$), h was total sensible heat transfer coefficient ($\mathrm{W/m^2/K}$), h_r was radiative heat transfer coefficient ($\mathrm{W/m^2/K}$), T_{sk} was skin surface temperature (℃), T_r was mean radiant temperature (℃).

Since there was no artificial light source during the experiment, which allows us to further equate the mean radiant temperature to the surrounding air temperature. Total sensible heat transfer coefficient (h) could be calculated as follow:

$$h = (h_c + h_r) = \frac{Q}{(T_{sk} - T_a)}, \quad (5)$$

We first measured total sensible heat transfer coefficient (h_0) of the unclothed manikin, and then the total sensible heat transfer coefficient of each segment when covering with adhesive

aluminium coating foil (h_{foil}). The emissivity of the foil was estimated as $\varepsilon = 0.025$, and the emissivity for the unclothed manikin was measured as $\varepsilon = 0.95$. Base on the assumption that h_c was the same with or without the foil covering, h_r can be calculated via:

$$h_0 - h_{foil} = h_{r0} - h_{rfoil} \tag{6}$$

$$\frac{h_{rfoil}}{h_{r0}} = \frac{0.025}{0.95} \tag{7}$$

where h_{r0} was the radiative heat transfer coefficient of the unclothed manikin ($\mathrm{W/m^2}/K$), h_{rfoil} was radiative heat transfer coefficient of each segment when covering with adhesive aluminium coating foil ($\mathrm{W/m^2}/K$).

By substituting h_{rfoil} in the equation, h_{r0} would be used as h_r for the following calculation:

$$h_{r0} = 1.027 \cdot (h_0 - h_{foil}) \tag{8}$$

Five different inflow velocity and three different turbulence intensity levels were tested in this study. The manikin experienced three different wind directions, including facing towards, facing backward and standing side on. The incoming flow approached from the front, sideway, and backway correspondingly. During the operation, we first turned on the manikin, and waited until it reached the thermal equilibrium status to adjust the speed of the fan to the targeted value. The time to reach equilibrium depended on different test conditions, and the 20-minute average value logged after equilibration was used for the following calculations.

3. Results and Discussion

3.1. General observations about the experiment results

The h_r results are shown in Table 2. The whole body radiative heat transfer coefficient in the present study is 4.6 ($\mathrm{W/m^2/}K$), which is in a good match with published estimates of 4.5 ($\mathrm{W/m^2/}K$) [29] and 4.3 ($\mathrm{W/m^2/}K$) [37]. The anatomical body segment findings reflect the theoretical estimation that the larger effective radiative area leads to larger radiative heat transfer coefficients, such as head, upper arm, and foreleg. The slight inconsistency in individual body segments may be due to different heights and surface areas of each body segment between different types of manikin. The largest discrepancy of 0.9 ($\mathrm{W/m^2/}K$) is observed for the manikin's head, which may be caused by their different hair-coverage. Instead of a shoulder-length hair adopted in the previous research [29], we have not put hair on our manikin for these experiments. Note that, to keep the manikin mechanically stable in the wind, her feet are anchored on the floor, and therefore the same posture is adopted when testing for h_r. To minimise the effect of conductive heat transfer, aluminium foam foil is used to separate the underneath of the feet and the floor surface. The contact surface area- the bottom of the feet- measured as 0.024 $\mathrm{m^2}$ has been subtracted from the total body area for the following calculation.

Table 2
Radiative heat transfer coefficient of 10 individual segments and whole body for the standing posture.

Manikin segment	h_r $(\mathrm{W/m^2}/K)$	
	Present study	de Dear et al. [29]
Foot	3.95	3.90
Calf	5.08	5.30
Thigh	4.57	4.30
Pelvis	4.51	4.20
Head	5.00	4.10
Hand	4.25	4.10
Forearm	4.39	4.90
Upper Arm	5.27	5.20
Chest	4.45	4.50
Back	4.52	4.40
Whole Body	4.60	4.50

3.2. Effect of wind velocity and direction

The whole body h_c increases from 13 $(\mathrm{W/m^2}/K)$ to 36 $(\mathrm{W/m^2}/K)$ as wind velocity increases to 5 m/s (see Fig. 3). The discrepancy between the left and right side of the manikin is caused by the slight difference in its position; i.e. the mechanical asymmetry of the shoulder joint leads to the different space between upper limbs and torso. Limbs always have higher h_c compared with torso [29]. For example, upper arms and chest are at the same height, which corresponds to the same incoming wind velocity and turbulence intensity; as the wind velocity changes from the lowest to the highest group, the difference in h_c between the upper arm and the chest gradually increases from 15% to 42%.

Under different wind azimuth angles, the whole body h_c are quite close, with the value for 'standing side-on' slightly lower, corresponding to the smallest windward area (see Fig. 3). With the wind blowing from the side (from the right of the manikin in this study), h_c on the left side of upper body; with the torso blocked in the medium, decreased by approximately 20% - 40% comparing with these on the right side. This trend is less obvious for the thigh and calf.

With the both facing torwards and backwards the wind, body segments directly contact with the upcoming wind experienced higher h_c compared to the corresponding segments that were facing downwind. When facing towards, the lowest h_c results are found in the leeward area, including the back left, back right and backside. However, in comparison between the back thigh and front thigh; back and chest, the relative increase of h_c is greater in the lee. The possible cause is the increasing turbulence intensity in the near wake flow behind the body segments.

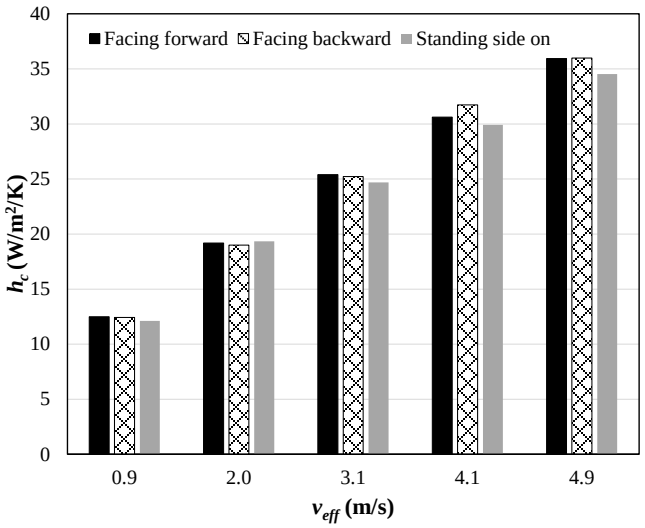

Fig. 3. Convective heat transfer coefficient for the standing manikin at medium TI group, with three approaching wind directions: facing torwards, facing backward, and standing side on.

3.3. Effect of turbulence intensity (TI)

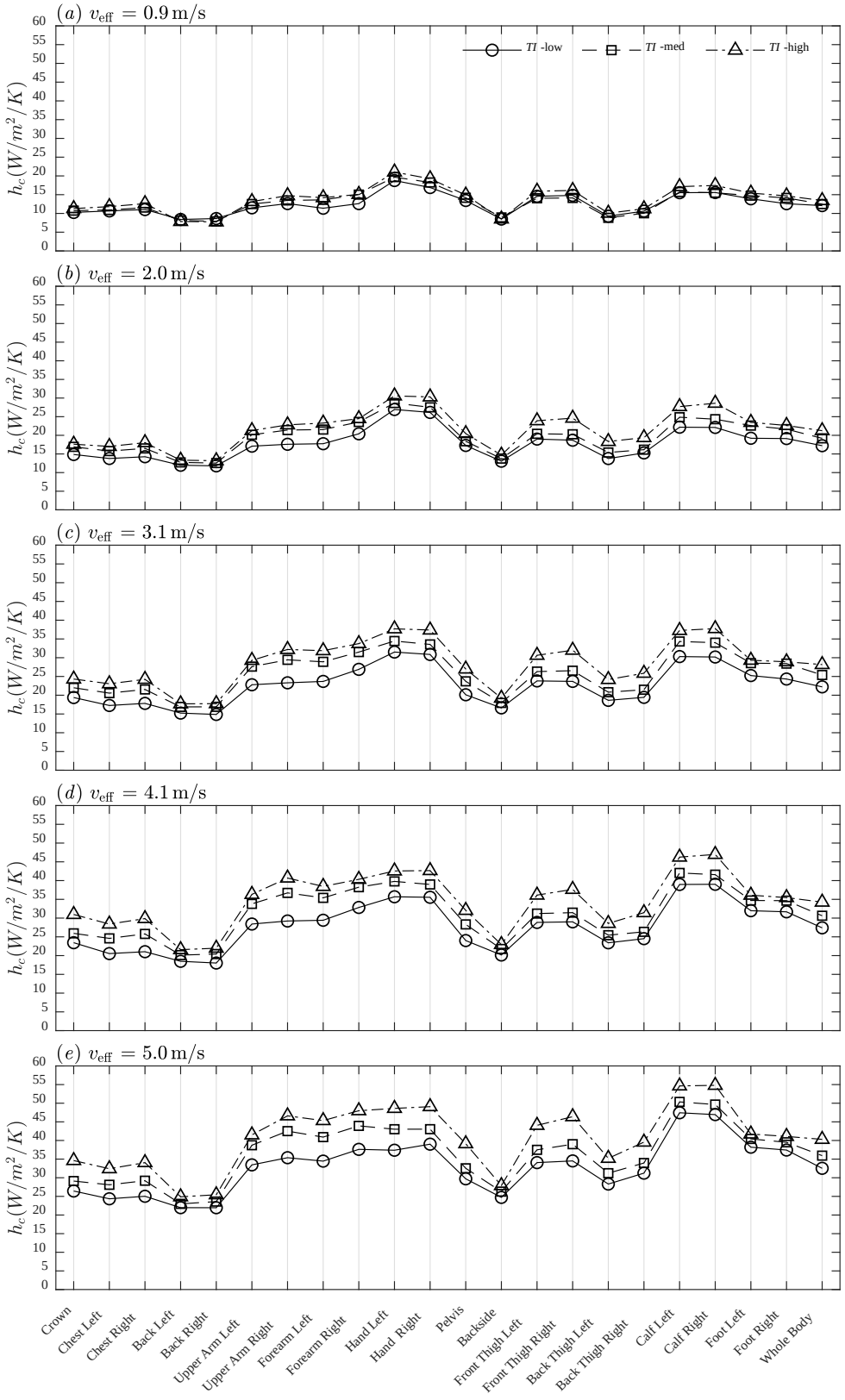

Fig. 4. (a) - (e) Convective heat transfer coefficients of 22 anatomical segments, plus whole body, facing towards the wind at three different *TI* conditions for different wind velocities.

The comparison of h_c at different turbulence intensities (each at five velocities) are shown in Fig.4 (a)-(e). The enhancing effect of turbulence intensity on convective heat transfer is readily discernible in these figures. For individual body segments, those on the leeward side, though sensitive to the change in wind velocity (as mentioned in the previous section), are less affected by the change in turbulence intensity. We calculate the unit effect of *TI* on h_c for whole body by $\frac{\Delta h_c}{\Delta TI}$, where $\Delta h_c = h_{c(\,TI_{high})} - h_{c(TI_{low})}$, $\Delta TI = TI_{high} - TI_{low}$. The results are shown in Fig. 5, where the horizontal line inside the box indicates the median; the circle indicates the mean; the box covers 25-75 percentiles; and the whisker extends to the extreme value without considering the outliers (beyond 1.5 times the interquartile range). The intensification effect of turbulence is greater in higher wind velocity, thus the trend flattens when $v_{eff} > 3$ m/s. When $v_{eff} = 0.9$ m/s, $\frac{\Delta h_c}{\Delta TI}$ on whole body is merely 0.1 ($W/\mathrm{m}^2/K$) (Note that *TI* is non-dimensional). Specifically, increasing the turbulence intensity from 15% to 30% results to an increase of 1.5 ($W/\mathrm{m}^2/K$) only in h_c. This finding agrees with that of Mayer [22], and reveals the reason why turbulence intensity has been conventionally ignored in the calculation of h_c for indoor environments, where the wind velocity is generally designed below 0.5 m/s. However, previous measurements in a public place [11] recorded a much higher wind velocity outdoors, with the transient wind velocity generally around 2-3 m/s. Under these circumstances, the same 15% growth in turbulence intensity will increase h_c with approximately 4.5 ($W/\mathrm{m}^2/K$) to 6.3 ($W/\mathrm{m}^2/K$), which almost accounts for one third of h_c, and not negligible. Body segments directly facing into the wind like the chest for example, were more sensitive to changing *TI* than the back, and the same relativity exists for pelvis and backside.

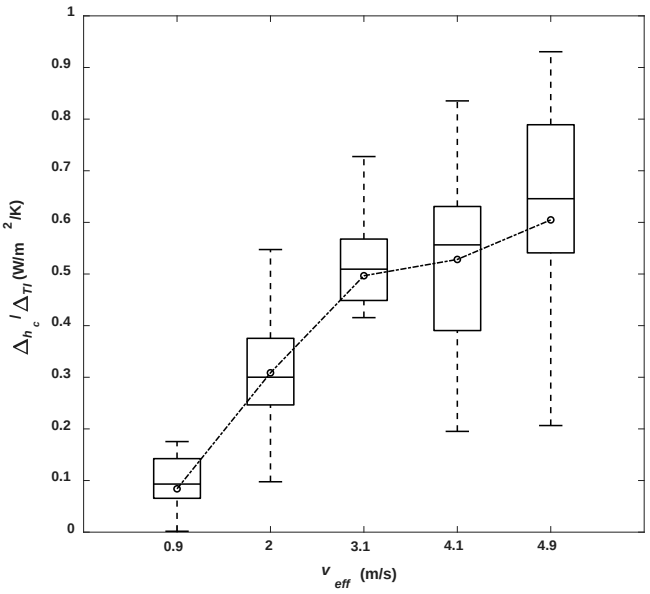

Fig. 5. The unit effect of *TI* on h_c for whole body.

3.4. Regression formula of convective heat transfer coefficient

The intensification effect of turbulence intensity and wind velocity on convective heat transfer over the manikin surface has been demonstrated in this study. The relationship between TI and h_c has been qualitatively assessed on simple geometries through experiments and simulations, and considering the most body segments (such as limbers and trunk) approximately as a cylinder or sphere, sharing the same principle of heat transfer, a formula for h_c could be constructed in a similar way. For cylinders, the intensification of heat transfer $\frac{Nu}{Nu_0}$ (Nu is the Nusselt number (the dimensionless parameter characterizing convective heat transfer), and Nu_0 is the value obtained for *TI* close to 0%) is usually described as a linear regression of the turbulent Reynolds number Re_T [38]:

$$\frac{Nu}{Nu_0} = 1 + B\ Re_T \tag{9}$$

where Re_T is the ratio of turbulent energy production and dissipation [39], classically approximated by $TI * Re^{0.5}$. Grisalberti et al. [40] found that body properties (shape, dimensions, and positions) have less influence on the heat transfer coefficient than flow properties, and the relationship between flow characteristics and heat transfer coefficient has been described by:

$$h = Au^n * (1 + B\ TI * u^{0.5}), \tag{10}$$

where *A* and *n* depend on the shape of the segments, while *B* is less affected. To obtain the coefficient estimates of *A* and *B*, we used the least-squares fitting method to minimize the sum of square of residuals.

Table 3
Forced convection for individual body segments - regression coefficient in Eq.10.

Segments	*A*	*B*	*n*	R^2
Head	7.14	1.99	0.45	0.996
Crown	9.09	1.58	0.48	0.996
Chest Left	8.17	1.48	0.44	0.994
Chest Right	8.22	1.73	0.42	0.994
Back Left	7.95	0.36	0.59	0.997
Back Right	7.57	0.48	0.59	0.995
Upper Arm Left	10.75	0.88	0.58	0.995
Upper Arm Right	10.21	1.43	0.55	0.993
Forearm Left	10.46	1.31	0.56	0.996
Forearm Right	12.53	0.89	0.57	0.996
Hand Left	16.90	0.98	0.35	0.991
Hand Right	15.81	0.94	0.41	0.989
Pelvis	10.21	1.41	0.42	0.995
Backside	8.38	0.34	0.63	0.986
Front Thigh Left	10.86	1.35	0.46	0.995
Front Thigh Right	9.98	1.78	0.46	0.990
Back Thigh Left	7.62	1.10	0.62	0.997
Back Thigh Right	7.74	1.34	0.61	0.998
Calf Left	11.13	0.65	0.65	0.996
Calf Right	10.96	0.79	0.63	0.996
Foot Left	11.20	0.55	0.56	0.994
Foot Right	10.64	0.55	0.54	0.995
Whole Body	9.93	1.03	0.54	0.997

The regression results and corresponding R^2 values are presented in Table 3. The proposed hypothesis is statistically significant with Probability (P) value smaller than the significant level 0.05; residuals independent of one another and randomly distributed around zero without a pattern or trend discovered.

Compared with most of the previously published h_c regression formula, velocity is the single independent variable and turbulence intensity usually ignored(Fig. 6). de Dear et al. [29] reported the mean value of *TI* from 4% to 8%, and the prediction results of the regression formula Eq. (10) agree with those results quite well when we set the turbulence intensity as 4%. In comparison with Ono et al. [31], the discrepancy continues to grow with wind velocity and exceeds 20% when the velocity is larger than 3 m/s. This may be because their experiment was carried out at the wind velocity under 2 m/s, while the later results at a higher wind velocity range was realised through simulation.

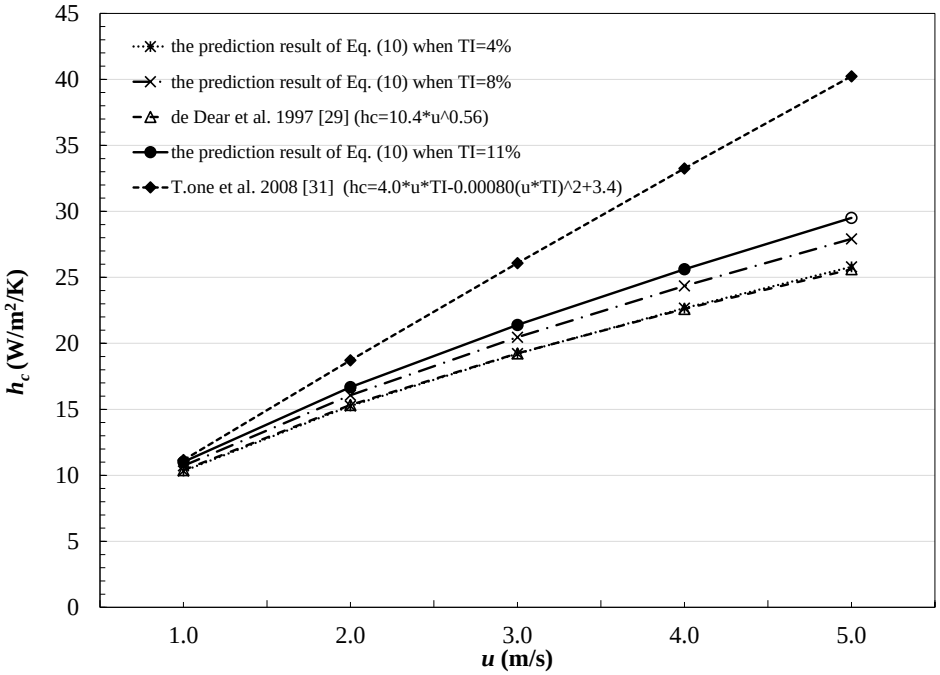

Fig. 6. Comparison of whole-body h_c in this study with previously published estimates.

3.6. Amended velocity input for the existing thermal comfort model

More work needs to be done before we fully understand the mechanism of turbulence intensity's impact on thermal comfort; one of our ongoing research activities using live human subjects aims to study the thermal-physiological effects. For now, we have proposed a user-side amendment on velocity input; i.e. replace the original wind speed with "equivalent velocity" (u_{equal}) which accounts for the integrated effect of wind velocity plus turbulence intensity on the final convective heat transfer. Here we choose one of the widest adopted outdoor thermal comfort index-Physiological Equivalent Temperature (PET) as an example. The h_c in PET has a form of $h_c = au^b$, where *a* and *b* are coefficients. The amended wind velocity is given as,

$$u_{equal} = \sqrt[1/b]{\frac{A*u^n*(1+B*TI*u^{0.5})}{a}} \tag{11}$$

We further investigate the sensitivity of thermal comfort index against turbulence intensity. Niu et al. [41] proposed a perceivable environmental parameter, defined as the difference in the meteorological parameter that can cause a significant difference in thermal perception; a 2.5 ℃ change in PET comparing with the comfort base condition ($T_a = T_r = 23℃$, $V_a = 0.1\ \mathrm{m}/s$). Thermally perceivable wind speed difference$\left(\Delta V_{a,0.5}\right)$ is -1.3 m/s without regard to turbulence intensity, and -0.7 m/s at *TI* = 30%. Specifically, with the same change in wind speed, under a higher turbulence intensity level, the effect of the wind speed has almost been underestimated by half.

4. Conclusions

This study confirms the intensifying effect of turbulence intensity on the convective heat loss from the human body surface. The convective heat transfer coefficient over different segments of a thermal manikin has been studied experimentally in simulated outdoor wind conditions in a boundary layer wind tunnel. The results show that when the wind speed is between 2-3 m/s, ignoring the turbulence intensity may underestimate the heat transfer coefficient by about 30%, and lead to the insensitivity of predicted results to the change of wind in thermal comfort model. A new set of regression formula can now be used to take the combined effect of wind velocity and turbulence intensity into the prediction of convective heat loss and may further contribute to the prediction of skin temperature and thermal sensation by numerical thermal-physiological simulation models [6-9].

Before it could be embedded into the existing thermal comfort models, we also provide users with a simple pre-treatment method for the wind input parameters. To better reflect the state of a real life condition, different clothing conditions, dynamic postures of the manikin and a more complex sweating situation relate with evaporative heat loss need to be tested and added into the model in the future.

To cover a full range of exposures at typical outdoor pedestrian-level wind conditions, experiments of the type described in the present paper are needed for higher turbulence levels. A further concern in practical utilization of these results is the absence of empirical field data for turbulence intensity at pedestrian level in urban settings, which makes us unable to deduce the wind condition corresponding to different body segments by measurement at a certain height above the ground. Our future research will include field measurement, focusing on how the shape of the wind profile under 2 m height changes with the surrounding urban morphology. Another avenue for further research is an experimental analysis of the effects of turbulence intensity on the latent heat losses from the human body in an urban outdoor setting.

Conflict of interest

The authors declare that there is no conflict of interest.

Acknowledgment

This research was supported by the School of Architecture, Design and Planning, and the School of Civil Engineering, both at The University of Sydney. The authors wish to thank Dr. Murali Krishna Talluru for assistance with hotwire anemometers, Mr. Theo Gresley-Daines, Mr. Zachary Benitez and Dr. Jing Xiong for their technical support in the wind tunnel manikin experiment. Students Mr. Jiwei Zou, Miss Yiwei Xia and Mr. Zixuan Chen are also thanked for their assistance during the experiments.

References

[1]M. Baccini, A. Biggeri, G. Accetta, T. Kosatsky, K. Katsouyanni, A. Analitis, H. R. Anderson, L. Bisanti, D. D'ippoliti, J. Danova, B. Forsberg, S. Medina, A. Paldy, D. Rabczenko, C. Schindler & P. Michelozzi, Heat Effects on Mortality in 15 European Cities, Epidemiology, 19 (2008) 711-719.
[2]J. Tan, Y. Zheng, X. Tang, C. Guo, L. Li, G. Song, X. Zhen, D. Yuan, A. J. Kalkstein, F. Li & H. Chen, The urban heat island and its impact on heat waves and human health in Shanghai, International Journal of Biometeorology, 54 (2010) 75-84.
[3]Y. Honda, M. Kondo, G. Mcgregor, H. Kim, Y.-L. Guo, Y. Hijioka, M. Yoshikawa, K. Oka, S. Takano, S. Hales & R. S. Kovats, Heat-related mortality risk model for climate change impact projection, Environmental Health and Preventive Medicine, 19 (2014) 56-63.
[4]D. Fiala, K. Lomas & M. Stohrer, A computer model of human thermoregulation for a wide range of environmental conditions: the passive system, Journal of Applied Physiology, 87 (1999) 1957-1972.
[5]D. Fiala, K. J. Lomas & M. Stohrer, Computer prediction of human thermoregulatory and temperature responses to a wide range of environmental conditions, International Journal of Biometeorology, 45 (2001) 143-159.
[6]P. Höppe, The physiological equivalent temperature – a universal index for the biometeorological assessment of the thermal environment, International Journal of Biometeorology, 43 (1999) 71-75.
[7]S. Tanabe, K. Kobayashi & J. Nakano, Evaluation of thermal comfort using combined multi-node thermoregulation (65MN) and radiation models and computational fluid dynamics (CFD), Energy & Buildings, 34 (2002) 637-646.
[8]D. Fiala, G. Havenith, P. Bröde, B. Kampmann & G. Jendritzky, UTCI-Fiala multi-node model of human heat transfer and temperature regulation, International Journal of Biometeorology, 56 (2012) 429-441.
[9]C. Huizenga, Z. Hui & E. Arens, A model of human physiology and comfort for assessing complex thermal environments, Building & Environment, 36 (2001) 691-699.
[10]T. Huang, J. Li, Y. Xie, J. Niu & C. M. Mak, Simultaneous environmental parameter monitoring and human subject survey regarding outdoor thermal comfort and its modelling, Building and Environment, 125 (2017) 502-514.

[11]Y. Xie, T. Huang, J. Li, J. Liu, J. Niu, C. M. Mak & Z. Lin, Evaluation of a multi-nodal thermal regulation model for assessment of outdoor thermal comfort: Sensitivity to wind speed and solar radiation, Building and Environment, 132 (2018) 45-56.
[12]Y. Xie, J. Liu, T. Huang, J. Li, J. Niu, C. M. Mak & T.-C. Lee, Outdoor thermal sensation and logistic regression analysis of comfort range of meteorological parameters in Hong Kong, Building and Environment, 155 (2019) 175-186.
[13]R. De Dear & J. Kim, Thermal Comfort Inside and Outside Buildings, *In:* TAMURA, Y. & YOSHIE, R. (eds.), Advanced Environmental Wind Engineering, Tokyo, Springer Japan, 2016, pp. 89-99.
[14]T. R. Oke, Boundary Layer Climates*,* 2nd Edition ed*,* Routledge, Lagos, 1987, pp. 33-42.
[15]J. Liu, J. Niu, Y. Du, C. M. Mak & Y. Zhang, LES for pedestrian level wind around an idealized building array—Assessment of sensitivity to influencing parameters, 44 (2018) 406-415.
[16]J. Liu, J. Niu, C. M. Mak & Q. Xia, Detached eddy simulation of pedestrian-level wind and gust around an elevated building, Building and Environment, 125 (2017) 168-179.
[17]M. R. Raupach, J. J. Finnigan & Y. Brunei, Coherent eddies and turbulence in vegetation canopies: The mixing-layer analogy, Boundary-Layer Meteorology, 78 (1996) 351-382.
[18]J. Liu & J. Niu, Delayed detached eddy simulation of pedestrian-level wind around a building array – The potential to save computing resources, Building and Environment, 152 (2019) 28-38.
[19]M. Roth, Review of atmospheric turbulence over cities, Quarterly Journal of the Royal Meteorological Society, 126 (2000) 941-990.
[20]J. C. R. Hunt, E. C. Poulton & J. C. Mumford, The effects of wind on people; New criteria based on wind tunnel experiments, Building and Environment, 11 (1976) 15-28.
[21]E. Mayer, Physical causes for draft: some new findings*,* 1987.
[22]E. Mayer, New measurements of the convective heat transfer coefficients: influences of turbulence, mean air velocity and geometry of human body, Proceedings of ROOMVENT, DANVAK, Aalborg, Denmark, 1992, pp. 263-276.
[23]E. Mayer, Assessment of draught by an artificial skin, Batiment international, Building research & practice, 17 (1989) 273-276.
[24]P. O. Fanger, A. K. Melikov, H. Hanzawa & J. Ring, Air turbulence and sensation of draught, Energy and Buildings, 12 (1988) 21-39.
[25]P. O. Fanger & N. K. Christensen, Perception of draught in ventilated spaces, Ergonomics, 29 (1986) 215-235.
[26]M. Kong, J. Zhang, T. Q. Dang, A. Hedge, T. Teng, B. Carter, C. Chianese & H. Ezzat Khalifa, Micro-environmental control for efficient local cooling: Results from manikin and human participant tests, Building and Environment, 160 (2019) 106198.
[27]D. P. Wyon, Use of thermal manikins in environmental ergonomics, Scandinavian Journal of Work, Environment & Health, 15 (1989) 84-94.
[28]S. Tanabe, H. Zhang, E. A. Arens, T. L. Madsen & F. S. Bauman, Evaluating thermal environments by using a thermal manikin with controlled skin surface temperature, Ashrae Transactions, 100 (1994) 39-48.
[29]R. J. De Dear, E. Arens, Z. Hui & M. Oguro, Convective and radiative heat transfer coefficients for individual human body segments, International Journal of Biometeorology, 40 (1997) 141-156.
[30]C. Li & K. Ito, Numerical and experimental estimation of convective heat transfer coefficient of human body under strong forced convective flow, Journal of Wind Engineering and Industrial Aerodynamics, 126 (2014) 107-117.
[31]T. Ono, S. Murakami, R. Ooka & T. Omori, Numerical and experimental study on convective heat transfer of the human body in the outdoor environment, Journal of Wind Engineering and Industrial Aerodynamics, 96 (2008) 1719-1732.
[32]A. Laneville. *Effects of turbulence on wind induced vibrations of bluff cylinders.* PhD Thesis, University of British Columbia, British Columbia, 1973.
[33]B. J. Vickery, Fluctuating lift and drag on a long cylinder of square cross-section in a smooth and in a turbulent stream, Journal of Fluid Mechanics, 25 (2006) 481-494.

[34]P. W. Bearman & T. Morel, Effect of free stream turbulence on the flow around bluff bodies, Progress in Aerospace Sciences, 20 (1983) 97-123.
[35]M. Fojtlín, J. Fišer & M. Jícha, Determination of convective and radiative heat transfer coefficients using 34-zones thermal manikin: Uncertainty and reproducibility evaluation, Experimental Thermal and Fluid Science, 77 (2016) 257-264.
[36]2013. ASHRAE handbook: fundamentals. SI ed. Atlanta, Georgia: American Society of Heating, Refrigerating and Air-Conditioning Engineers, Incorporation.
[37]M. Ichihara, M. Saitou, M. Nishimura & S.-I. Tanabe, MEASUREMENT OF CONVECTIVE AND RADIATIVE HEAT TRANSFER COEFFICIENTS OF STANDING AND SITTING HUMAN BODY BY USING A THERMAL MANIKIN, Journal of Architecture and Planning (Transactions of AIJ), 62 (1997) 45-51.
[38]A. Kondjoyan & J. D. Daudin, Effects of free stream turbulence intensity on heat and mass transfers at the surface of a circular cylinder and an elliptical cylinder, axis ratio 4, International Journal of Heat and Mass Transfer, 38 (1995) 1735-1749.
[39]D. Biswas & Y. Fukuyama, Calculation of Transitional Boundary Layers With an Improved Low-Reynolds-Number Version of the k–ε Turbulence Model, Journal of Turbomachinery, 116 (1994) 765-773.
[40]L. Ghisalberti & A. Kondjoyan, Convective heat transfer coefficients between air flow and a short cylinder. Effect of air velocity and turbulence. Effect of body shape, dimensions and position in the flow, Journal of Food Engineering, 42 (1999) 33-44.
[41]J. Niu, J. Liu, T.-C. Lee, Z. Lin, C. Mak, K.-T. Tse, B.-S. Tang & K. C. S. Kwok, A new method to assess spatial variations of outdoor thermal comfort: Onsite monitoring results and implications for precinct planning, Building and Environment, 91 (2015) 263-270.